

2016

Water residence time in Chesapeake Bay for 1980-2012

JB Du

Virginia Institute of Marine Science

Jian Shen

Virginia Institute of Marine Science

Follow this and additional works at: <https://scholarworks.wm.edu/vimsarticles>



Part of the [Aquaculture and Fisheries Commons](#)

Recommended Citation

Du, JB and Shen, Jian, "Water residence time in Chesapeake Bay for 1980-2012" (2016). *VIMS Articles*. 787.

<https://scholarworks.wm.edu/vimsarticles/787>

This Article is brought to you for free and open access by the Virginia Institute of Marine Science at W&M ScholarWorks. It has been accepted for inclusion in VIMS Articles by an authorized administrator of W&M ScholarWorks. For more information, please contact scholarworks@wm.edu.

1 Water residence time in Chesapeake Bay for 1980-2012

2

3 Jiabi Du, Jian Shen

4

5

6 Virginia Institute of Marine Science, The College of William and Mary, Gloucester Point,

7 VA 23062, USA

8

9 Corresponding author:

10

11 Jiabi Du, Virginia Institute of Marine Science, The College of William and Mary,

12 Gloucester Point, VA 23062, USA. (jiabi@vims.edu; jiabi.du@gmail.com)

13

14

15 **Abstract:** Concerns have grown over the increase of nutrients and pollutants discharged
16 into the estuaries and coastal seas. The retention and export of these materials inside a
17 system depends on the residence time (RT). A long-term simulation of time-varying RT
18 of the Chesapeake Bay was conducted over the period from 1980 to 2012. The 33-year
19 simulation results show that the mean RT of the entire Chesapeake Bay system ranges from
20 110 to 264 days, with an average value of 180 days. The RT was larger in the bottom
21 layers than in the surface layers due to the persistent stratification and estuarine
22 circulation. A clear seasonal cycle of RT was found, with a much smaller RT in winter
23 than in summer, indicating materials discharged in winter would be quickly transported
24 out of the estuary due to the winter-spring high flow. Large interannual variability of the
25 RT was highly correlated with the variability of river discharge ($R^2=0.92$). The monthly
26 variability of RT can be partially attributed to the variability of estuarine circulation. A
27 strengthened estuarine circulation results in a larger bottom influx and thus reduces the
28 RT. Wind exerts a significant impact on the RT. The upstream wind is more important in
29 controlling the lateral pattern of RT in the mainstem.

30

31 **Key words:** residence time, Chesapeake Bay, water exchange, estuarine circulation, wind,
32 river discharge

33

34

35 **1.Introduction**

36 Concerns have grown over the increase of nutrients and other pollutants discharged
37 into the estuaries and coastal seas(Nixon, 1995; Paerl et al., 2006; Smith et al., 1999).
38 These substances have deleterious effects on aquatic organisms and human health
39 through the food chain (Kennish, 1997). Due to the increase of anthropogenic nutrient
40 input, many estuaries and coastal seas have become more eutrophic over the past few
41 decades (Carpenter et al., 1998; Kemp et al., 2005; Murphy et al., 2011; Nixon, 1995).
42 The ecological responses of a waterbody to increased nutrient loads have been widely
43 linked to the flushing capability of the system (Boynton et al., 1995; Josefson and
44 Rasmussen, 2000; Monbet, 1992). The available nutrient supply for algae growth and
45 bloom is determined not only by the nutrient loads, but also by the retention of nutrients,
46 which is related to the residence time (RT) of a system (Nixon et al., 1996). For example,
47 coastal eutrophication has been built up in Koljo Fjords because of slow water exchange,
48 even though there are no significant nutrient loads (Lindahl et al., 1998; Nordberg et al.,
49 2001; Rosenberg, 1990). The export rate of nutrients proved to be strongly negatively
50 related with the RT(Dettmann, 2001; Nixon et al., 1996). The RT is thus a key parameter
51 in quantifying the impact of hydrodynamics on biochemical processes in an estuary
52 (Boynton et al., 1995; Cerco and Cole, 1992).In addition, from a management perspective,
53 it is essential to know the timescale for a pollutant discharged into a water body to exit
54 the system. Therefore, it is of importance to study the flushing capacity and water
55 exchange for an estuary.

56 To quantify the flushing capacity, several transport timescales have been used. Among
57 them, flushing time, RT, and water age are the three fundamental concepts of transport

58 time (Alber and Sheldon, 1999; Bolin and Rodhe, 1973; Hagy et al., 2000; Huang et al.,
59 2010; Liu et al., 2004; Liu et al., 2008; Shen and Haas, 2004; Shen and Wang, 2007).
60 Flushing time is regarded as a bulk or integrative property that describes the overall
61 exchange or renewal capability of a waterbody (Dyer, 1973; Geyer et al., 2000; Officer,
62 1976; Oliveira and Baptista, 1997). The age of a water parcel is defined as the time
63 elapsed since the parcel departed the region in which its age is defined to be zero
64 (Deleersnijder et al., 2001; Takeoka, 1984; Zimmerman, 1976). The RT of a water parcel
65 is defined as the time needed for the water parcel to reach the outlet (Zimmerman,
66 1976) and thus can be regarded as the remainder of the lifetime of a water parcel in a
67 waterbody (Takeoka, 1984). Age and RT can be applied not only to steady-state cases, but
68 also to time-varying cases (Deleersnijder et al., 2001; Delhez, 2005; Takeoka, 1984).
69 Although flushing time can be used to estimate the overall flushing capability of a
70 waterbody, the steady-state approach does not provide spatial and temporal variations in
71 a large estuary, especially in a partially mixed estuary (e.g., Chesapeake Bay), where the
72 transport could vary substantially in different regions and different vertical layers. The
73 transport process for a substance in an estuary has large variability due to the time-
74 varying estuarine dynamics. It is desirable to know the spatial pattern of the RT and its
75 temporal variation, which can be applied to determine the impact of hydrodynamics on
76 biogeochemical processes and be used for environmental assessment.

77 The water RT of Chesapeake Bay, the largest estuary in the United States, was not
78 well documented. The RT of the Bay's tributaries was calculated using box model or e-
79 folder time (e.g., Hagy et al., 2000; Shen and Haas, 2004). Hagy et al. (2000) calculated
80 the RT in Patuxent River, one main tributary of Chesapeake Bay, using a box model and

81 found the control of residence time from the head to its mouth changed from primarily
82 river flow to the intensity of gravitational circulation. The spatially averaged RT of 7.6
83 months in Chesapeake Bay was estimated in a numerical model using e-folder
84 time(Nixon et al., 1996). The spatial pattern of transport time in the Bay's mainstem was
85 initially investigated by Shen and Wang (2007) using the concept of freshwater age.
86 They found that it requires 120-300 days for a marked change in the characteristics of the
87 pollutant source discharged into the Bay from the Susquehanna River to affect
88 significantly the conditions near the Bay mouth for selected wet and dry years. However,
89 the spatial variation and long-term temporal variation of the RT still remained largely
90 unknown.

91 Here we aim to investigate the spatial pattern and long-term temporal variability of the
92 RT in Chesapeake Bay. A long-term numerical simulation of the RT from 1980 to 2012
93 in Chesapeake Bay was conducted for the first time using a robust algorithm developed
94 by Delhez et al. (2004). The seasonality and interannual variability of RT will be
95 examined. Finally, the main factors controlling the variation of RT will be discussed,
96 including river discharge, estuarine circulation and wind.

97 **2. Methods**

98 **2.1 RT calculation**

99 The RT is often computed using a particle tracking method by injecting some particles
100 at a fixed time, following the path of these particles, and registering the time when they
101 leave the domain of interest (Gong et al., 2008; Monsen et al., 2002). Another method to
102 calculate the RT is to use the remnant function approach proposed by Takeoka(1984), by

103 integrating the model-calculated tracer concentration timeseries to give a mean RT(Wang
 104 et al., 2004; Wang and Yang, 2015). With both approaches, the RT depends on the
 105 release time and different values of RT will be obtained if particles or tracers are released
 106 at different times, such as high tide or low tide (Brye et al., 2012).In order to obtain a
 107 mean RT for a period, many releases are required with regard to the changing current
 108 condition (Monsen et al., 2002). They are not computationally efficient, and therefore it
 109 is difficult to evaluate the long-term temporal variation of RT. Delhez et al. (2004)
 110 proposes an adjoint method to compute the RT. The method provides variations of RT in
 111 space and time with a single model run. The method does not require any Lagrangian
 112 module. It is based on an Eulerian algorithm that makes it more appropriate for long-term
 113 and large-scale simulations than the straightforward Lagrangian approach (Delhez, 2005).

114 According to the approach of Delhez et al.(2004), the mean RT,denoted by θ as a
 115 function of time t and location x , can be computed using the adjoint equation expressed as,

$$116 \quad \frac{\partial \overline{\theta(t, x)}}{\partial t} + \delta_{\omega}(x) + v \cdot \nabla \overline{\theta(t, x)} + \nabla \cdot [\kappa \cdot \nabla \overline{\theta(t, x)}] = 0 \quad (1)$$

117 where v is the velocity vector, κ is the symmetric diffusion tensor and

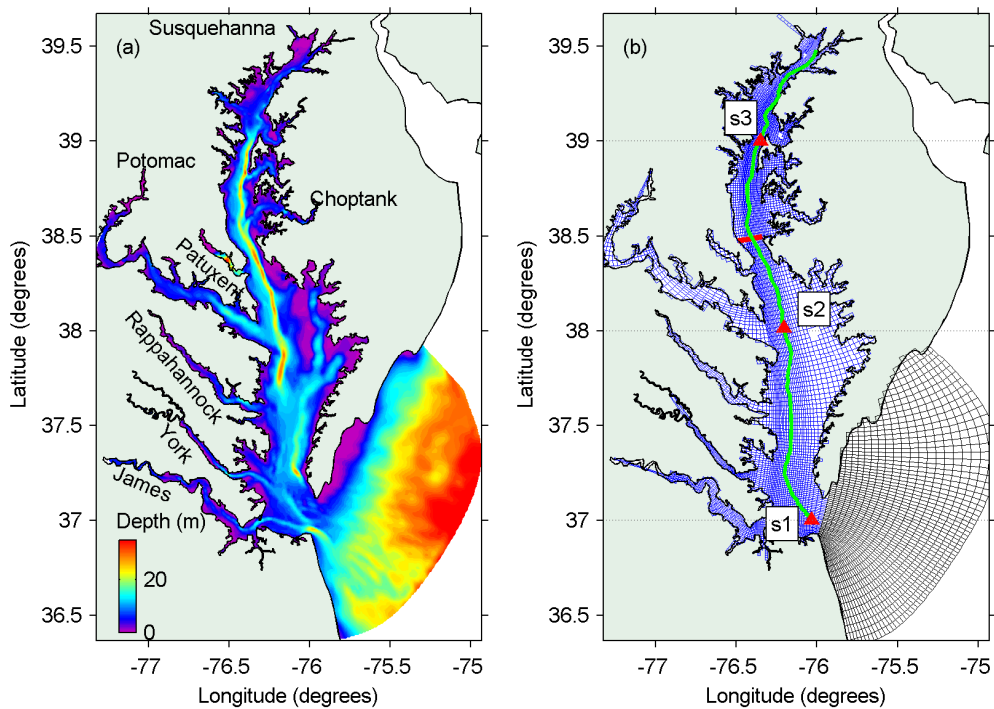
$$118 \quad \delta_{\omega}(x) = \begin{cases} 1 & \text{if } x \in \omega \\ 0 & \text{if } x \notin \omega \end{cases} \quad (2)$$

119 where ω is the domain of interest. At the boundary of the domain of interest $\theta = 0$ is
 120 used, which ensures the residence time to vanish at the boundary for the first time the
 121 water parcel hits the boundary and the computed residence time is the same as the
 122 residence time computed using Lagrangian method (Delhez and Deleersnijder, 2006;

123 Blaise et al., 2010). For stability reasons, the adjoint equation must be integrated
124 backward in time with the reversed flow, i.e. velocity vector v changed to $-v$. The
125 backward procedure is also necessary because one does not know in advance the fate of
126 the particles (Delhez, 2005). In order to calculate the mean RT, two steps were required.
127 In the first step, the hydrodynamic model was used to generate the velocity and
128 turbulence fields, and the intermediate results were saved every half-hour. We ran a
129 hydrodynamic model from 1979 to 2014 and obtained 35 years (1980-2014) of
130 hydrodynamic fields. The first year of 1979 was used to spin-up the model and not used
131 to calculate the RT. In the second step, Eq. 1 was integrated backward with the
132 interpolated hydrodynamic field at each time step based on the hydrodynamic field saved
133 in the first step, running from the end of 2014 to the beginning of 1980. The model
134 experiments showed that it takes about 1.5 years for the RT to reach a stable value in
135 Chesapeake Bay. Therefore, results of RT in the last two years (i.e., 2013 and 2014) were
136 not used and only the RT values of 1980-2012 were used for analysis.

137 In this study, we set the boundary of the domain of interest at the mouth of the Bay
138 and computed the RT at any location x and time t inside the Bay. $\theta(t, x) = T$ denotes that
139 particles released at location x and time t will be transported to the mouth of the Bay for a
140 period of T . In other words, RT is determined by the hydrodynamics after the release.
141 Notes that the domain of interest in this study included the tributaries (Fig. 1b). As
142 freshwater discharges into estuary at its headwater, which would lead to a non-zero RT
143 value at the headwater due to the fact that water parcels released at the headwater of
144 tributaries will not return and hit the upstream boundary.

145 **2.2 Simulation of the hydrodynamics**



147

148 **Fig. 1.** (a) Bathymetry of the numerical model; (b) domain of interest (blue grid), the
 149 deep channel section (green line), middle Bay cross-section (red line), and Station s1, s2
 150 and s3 (red triangle)

151

152 A numerical model based on the Environmental Fluid Dynamics Code (EFDC)
 153 (Hamrick, 1992) was used to simulate the hydrodynamics. EFDC uses a boundary-fitted
 154 curvilinear grid in the horizontal and sigma grids in the vertical. The EFDC model used
 155 for the Chesapeake Bay was also referred to as the HEM-3D model (Hong and Shen,
 156 2012, 2013; Du and Shen 2015). The same model was used for this study with the same
 157 model configuration and boundary condition. A grid with a horizontal dimension of
 158 112×240 and 20 layers in the vertical was deployed (Fig. 1). The model was forced by

159 interpolated observed tide at the open boundary (<http://tidesandcurrents.noaa.gov>),
160 freshwater discharges of eight main tributaries (<http://waterdata.usgs.gov/nwis/>), and
161 wind obtained from the North American Regional Reanalysis (NARR) produced at the
162 National Center for Environmental Prediction
163 (<http://www.esrl.noaa.gov/psd/thredds/catalog/Datasets/NARR/pressure/catalog.html>). This
164 model has been calibrated for tidal and non-tidal surface elevation, current, and salinity
165 for the Chesapeake Bay from 1999-2008 and it has simulated reliable stratification and
166 destratification responses temporally and spatially in both wet and dry years (Hong and
167 Shen, 2012, 2013). Details of model calibration can be found in Hong and Shen (2012).
168 We ran the model from 1979 to 2014, and saved the half-hourly hydrodynamic results,
169 which were then used to calculate the RT with the method described above.

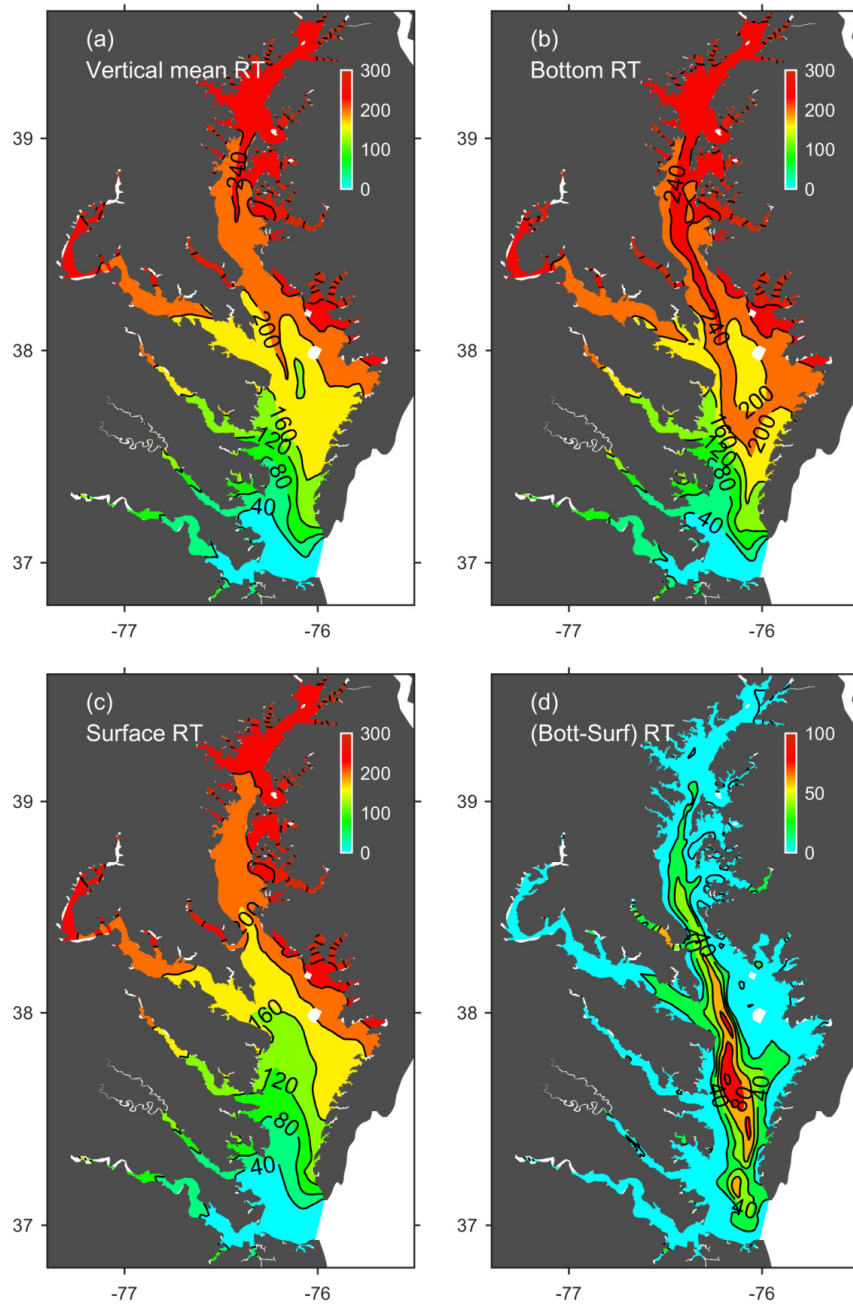
170 **3. Results**

171 **3.1 Mean RT of Chesapeake Bay**

172 The mean RT of Chesapeake Bay averaged over the period from 1980 to 2012 is
173 presented in Fig. 2. The spatially and vertically averaged RT value of the entire
174 Chesapeake Bay system for 1980-2012 was 180 days, shorter than 7.6-month reported in
175 Nixon et al. (1996). It was larger than the flushing time estimated by calculating the ratio
176 of freshwater volume to freshwater flow, which ranged from 90 to 140 days (Goodrich,
177 1988; Kemp et al., 2005; Shen and Wang, 2007). The difference was due to the fact that
178 the flushing time estimation in previous studies was actually the mean renewal time of
179 freshwater while the RT in this study included renewal of both the freshwater and saline
180 water. Hong and Shen (2012) estimated the RT by releasing dye at the beginning of the

181 model run and using the e-folder method to determine the RT for a typical mean flow
182 year. Their results suggested that the mean RT in a mean flow year was about 175
183 days, which is consistent with our results.

184



185

186 **Fig. 2.** Vertical mean (a), bottom (b), and surface (c) residence time (days) averaged
187 over 1980-2012; (d) difference between the bottom and surface residence time, positive
188 denoting larger residence time in bottom layers.

189

190 Considering the entire Chesapeake Bay as a box, the ratio of total water volume V to the
191 mean residence time T_R can be regarded as the total effective outflow of the system, Q_{out} .
192 For a steady state condition, the total effective outflow should equal the total influx of
193 “clean” water, which has two sources, river freshwater discharge R and influx of “clean”
194 water from the outside of the Bay Q_{in} . Here the clean water from the outside of the Bay
195 refers to the water that was not transported out of the Bay during the previous ebb tide.

196
$$Q_{out} = V/T_R = Q_{in} + R \quad (3)$$

197 Based on the simulation of the past 3 decades, the mean Q_{out} is about 4800 m³/s, given
198 the volume of the entire Chesapeake Bay system V of 7.5×10^{10} m³ and T_R of 180 days. The
199 total mean freshwater discharge from all the rivers R was about 2200 m³/s. Therefore,
200 Q_{in} is about 2800 m³/s, which is of the same order of magnitude as the influx at the Bay
201 mouth measured by Wong and Valle-Levinson (2002). This estimation suggests that the
202 influx of coastal ocean water is as equally important as the freshwater discharge on the
203 water renewal in Chesapeake Bay.

204 There was a clear longitudinal pattern of the RT. The vertical mean RT ranges from 0
205 to 200 days in the lower Bay (37-38N), 200-240 days in the middle Bay (38-39N), and
206 240-280 days in the upper Bay (39-39.6N) (Fig. 2a). The gradient of RT was larger in the

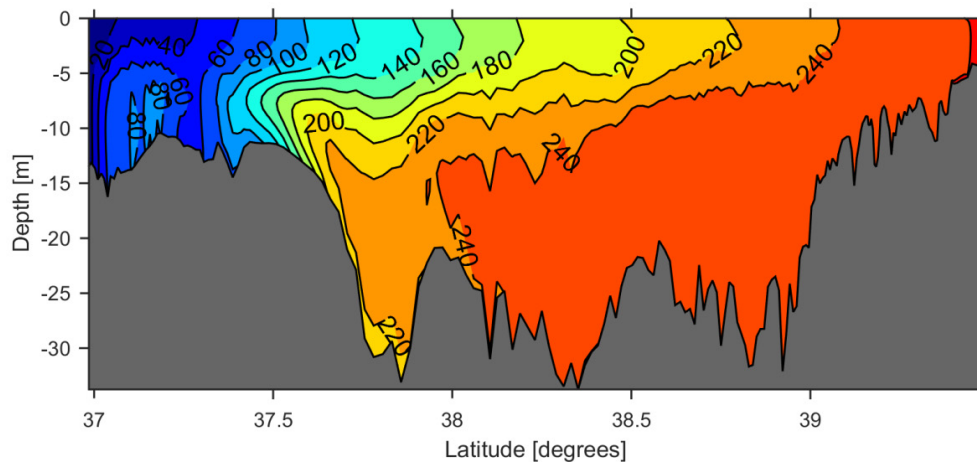
207 lower Bay than that in the middle-upper Bay. It took about 200 days to transport a water
208 parcel from the Potomac River mouth (~38N) to the Bay mouth (~37N), while it took
209 only 260 days to transport a parcel from the head of the Bay (~39.5N) to the Bay mouth.

210 The lateral distribution of vertical mean RT was different in different regions. The
211 lateral asymmetry of the vertical mean RT in the lower Bay was significant, with a much
212 larger RT in the eastern bank than that in the western bank (Fig. 2a). The difference could
213 be as large as 80 days. The lateral asymmetries could be attributed to several factors, such
214 as lateral shearing of the gravitational circulation (Valle-Levinson et al., 2003), the
215 large freshwater discharge from the western tributaries (e.g., Potomac River, York River,
216 and James River), and the strengthened ebb flow along the western boundary due to
217 Coriolis force. The lateral pattern was similar in both surface and bottom layers in the
218 lower Bay. In the middle to upper Bay, the vertical mean RT was larger in the deep area
219 than in the shallow region, which was caused by a larger bottom RT in the deep channel
220 due to the typical gravitational circulation with flow in the deep channel directed to the
221 upstream.

222 The vertical pattern of the RT can be examined by averaging the RT for the surface and
223 the bottom, respectively (Figs. 2b, 2c). The surface RT is the RT averaged over the 5
224 layers near the surface, and the bottom RT is the RT averaged over the 5 layers near the
225 bottom. The bottom and surface RT, and their difference were presented in Figs. 2b-d,
226 and the vertical profile along the deep channel section was shown in Fig. 3. The gradient
227 of RT was much larger in the bottom layers than in the surface layers, especially in the
228 deep channel section (Figs. 2, 3). The mean bottom RT of the Bay's main stem was about
229 184 days and the mean surface RT was about 145 days. There were minor vertical

230 differences in the upper Bay and shallow banks, where the water was well-mixed and the
231 vertical difference was less than 10 days (Fig. 2d). Vertical differences were significant in
232 the lower to middle Bay, especially in the deep channel where differences had a range of
233 20-100 days. The maximum vertical difference was found in the deep channel outside of
234 the Rappahannock River mouth ($\sim 37.75^{\circ}\text{N}$).

235



236

237 **Fig. 3.** Vertical profile of residence time (days) along the deep channel section.

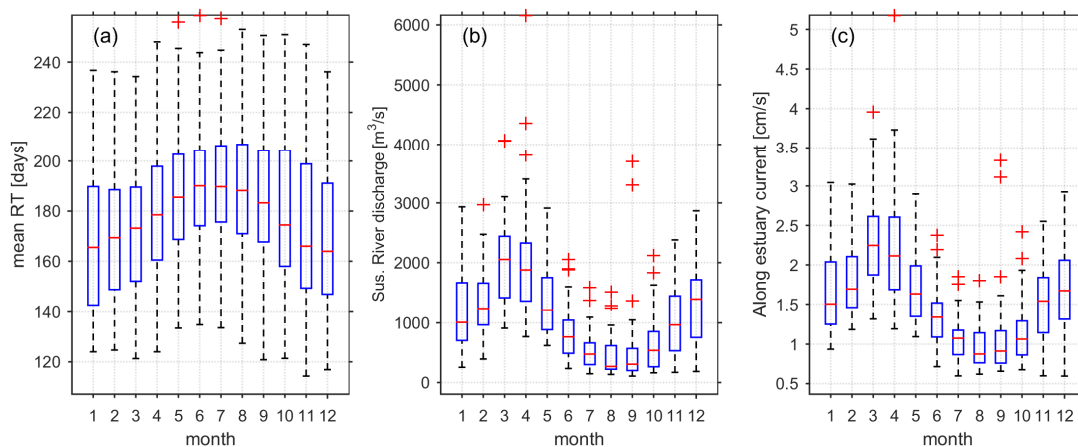
238

239 3.2 Seasonal cycle of RT

240 The vertical mean RT of the entire Bay exhibited a clear seasonal cycle, with its largest
241 value in summer (Jun.-Aug.) and smallest value in Nov.-Jan. This seasonal cycle
242 suggested that winter has a short retention time for soluble materials. In contrast, material
243 released in the summer usually has the longest retention time in the Bay. The minimum
244 RT during the winter was mainly due to large freshwater discharge during ensuing

245 months (e.g. Mar. and Apr.), which caused a large downstream residual current during
 246 this high-flow period (Fig. 4b-c). Taking Susquehanna River as an example, the river
 247 discharge usually peaked in March and troughed in August, which was consistent with
 248 the downstream residual current averaged over the Bay's mainstem.

249



250

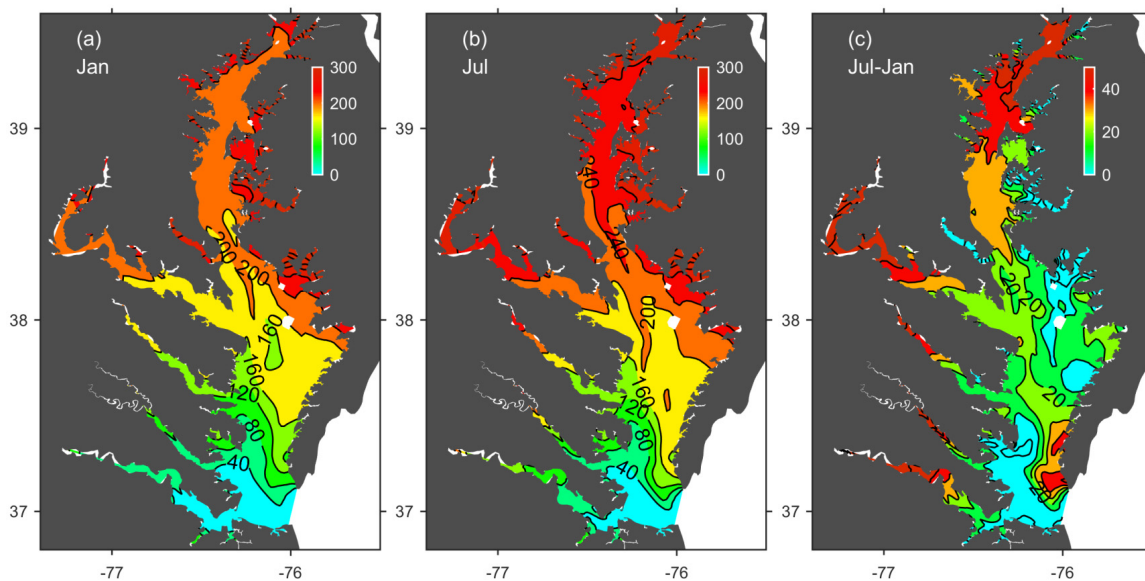
251 **Fig. 4.** (a) Seasonal cycle of residence time averaged over the entire Bay; (b) seasonal
 252 cycle of Susquehanna River flow; (c) seasonal cycle of vertically mean residual along
 253 estuary current averaged over the Bay's mainstem. Red lines denote medians of the 33
 254 years of record from 1980 to 2012, blue rectangles denote the first and third quartiles,
 255 dashed lines denote the upper and lower whiskers, and red crosses denote the outliers.

256

257 RT values during January and July were selected to represent the seasonal minimum and
 258 maximum RT (Fig. 5a-b). In the middle to upper Bay, a small area had RT values larger
 259 than 240 days in January (Fig. 5a), while the major area had RT values exceeding 240
 260 days and some areas had RT even exceeding 280 days in July (Fig. 5b). The difference

261 between July and January RT could be larger than 50 days in the upper Bay, 20-40 days in
262 the middle Bay, and 0-40 days in the lower Bay (Fig. 5c). The seasonal difference was
263 highly asymmetrical between the eastern and western banks in the lower Bay (Fig. 5c).
264 The seasonal difference along the western bank of the lower Bay was usually less than 10
265 days, but it could be as large as 40 days along the eastern bank. A similar pattern of
266 seasonal difference was found for both bottom and surface layers (not shown). Little
267 seasonal difference of the RT in the western bank of the lower Bay was related to the
268 dominating role of frequent tidal exchange in this area. The tidal current (0-100 cm/s) had
269 a much larger magnitude than the residual current (1-2.5 cm/s, Fig. 4c) induced by the
270 river discharge. The dominating ebb current and large influence of the tide caused the
271 persistently small RT and little seasonal difference along the western bank near the Bay
272 mouth. The tidal effect decreased in the middle and upper Bay, where the river discharge
273 became more influential on the variation of RT.

274



275

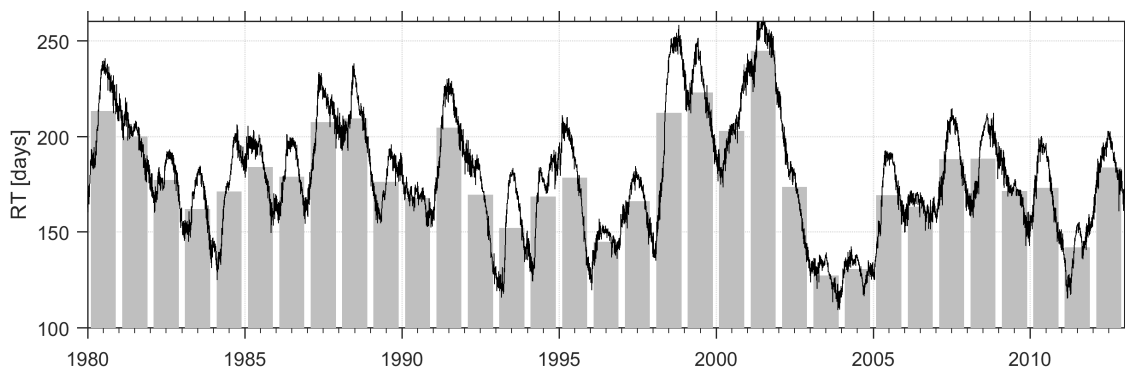
276 **Fig. 5.** Vertical mean residence time (days) averaged over 1980-2012 in January (a)
277 and July (b); (c) difference between July and January vertical mean residence time,
278 positive value denoting larger residence time in July.

279

280 3.3 Interannual variation of RT

281 There was high interannual variability of the RT. The vertical mean RT of the entire
282 Bay had a standard deviation of 30 days over the period of 1980-2012. The maximum
283 and minimum of the vertical mean RT averaged over the entire Bay were 264 days and
284 110 days, respectively (Fig. 6). No significant trend of the RT was found during the past 3
285 decades. There were several particularly high RT years with a yearly mean RT larger than
286 200 days, e.g., 1980, 1987, 1988, 1991, 1998, 1999, 2000 and 2001 (Fig. 6). The
287 maximum RT occurred in 2001, and the minimum RT occurred in 2003-2004.

288



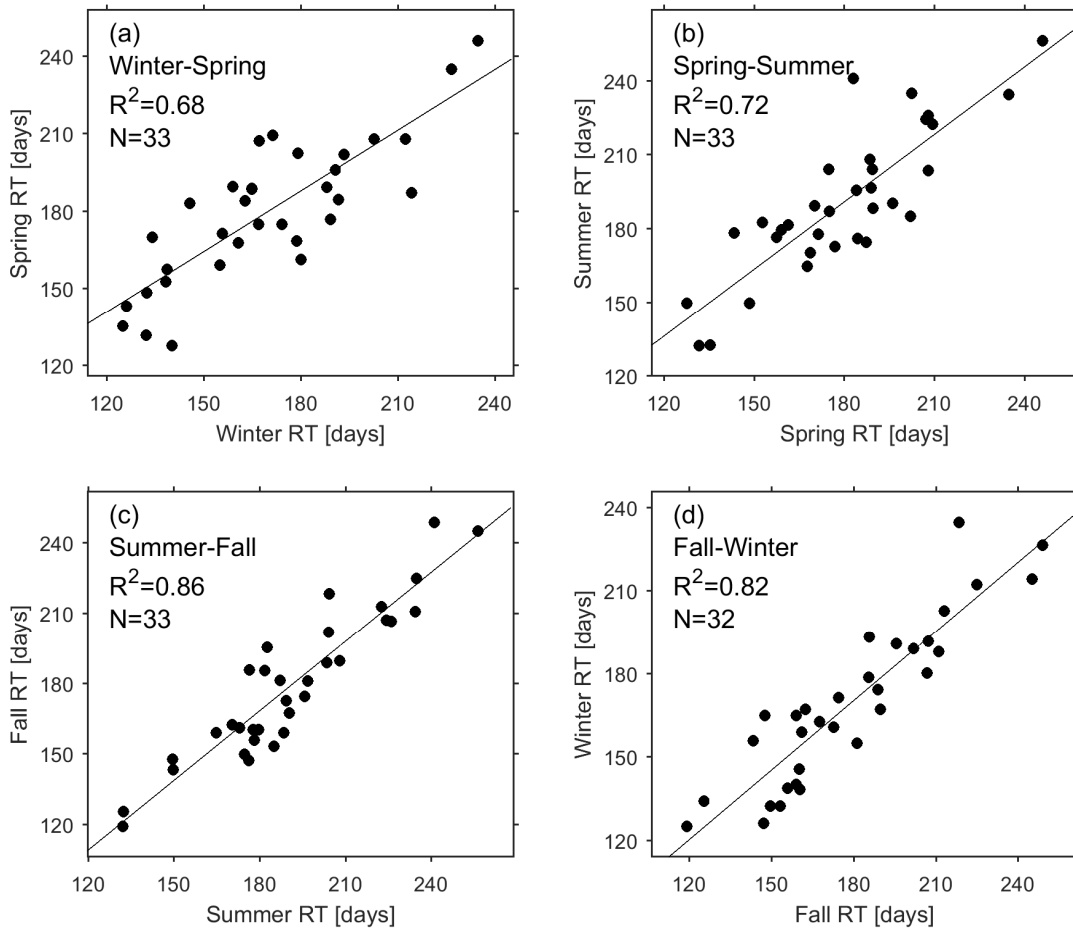
289

290 **Fig. 6.** Time series of vertical mean residence time averaged over the entire Bay for
291 1980-2012; bar plot indicates the yearly mean.

292

293 Since the RT highly depends on sub-tidal transport processes, the status of the
294 stratification, and the residual current field, we hypothesized that part of the RT variation
295 was related to the pre-existing condition. Regressions between the RT of a given season
296 and the RT of the following season were conducted. The regressions demonstrated that
297 the interannual variation of the previous season accounted for a large portion of
298 interannual variation of the RT in the following season (Fig. 7). However, the impact of
299 the pre-existing condition varied from season to season. A stronger effect of the pre-
300 existing condition occurred in the fall and winter with an R^2 value larger than 0.82,
301 followed by summer with an R^2 value of 0.72. The effect of the pre-existing condition was
302 relatively weaker in the spring, as the winter RT variation accounted for only 68% of
303 spring RT variation. The weaker effect of the pre-existing condition in the spring could
304 be attributed to the high variability of the spring river discharge.

305



306

307 **Fig. 7.**Regression of the residence time between winter and spring (a), spring and
 308 summer (b), summer and fall (c), fall and winter (d). The linear regression coefficient is
 309 shown in text.Spring (Mar.-May), summer (Jun.-Aug.), fall (Sep.-Nov.), and winter
 310 (Dec.-Feb.).

311

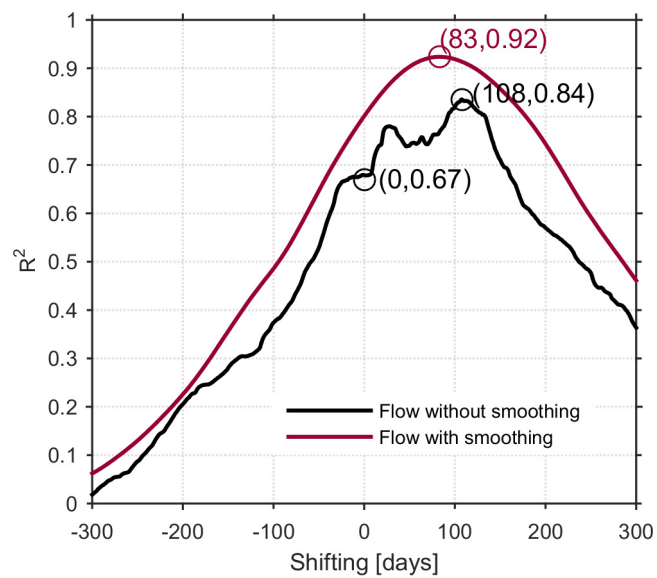
312 4. Discussion

313 4.1 Relationship between RT and river flow

314 Even though the variation of RT is generally believed to be highly controlled by
 315 the river discharge (Hagy et al., 2000; Shen and Haas, 2004), it is of interest to examine

316 the relative importance of river discharge on the RT over different timescales (e.g.
317 monthly, yearly), and to examine the mean delay between RT and river discharge. We
318 chose the river discharge of Susquehanna River to represent the total river discharge,
319 since the discharge of Susquehanna River accounts for 51% of the total discharge and
320 river discharges from other rivers are usually proportional to it (Guo and Valle-Levinson,
321 2007). The Susquehanna River daily discharge time series was extracted from the USGS
322 website (<http://waterdata.usgs.gov/nwis>). The linear regression between the yearly mean
323 RT and the inverse of the yearly mean river flow (without smoothing) has a correlation
324 coefficient R^2 of 0.67 (Fig. 8).

325



326

327 **Fig.8.** Linear regression coefficient R^2 between the interannual variation of vertical
328 mean residence time averaged over the entire Bay and the interannual variation of shifted
329 Susquehanna River flow, x-axis denoting the shifting days of flow.

330

331 To estimate the delay between river flow and RT, a series of regressions between the
332 yearly mean RT and the inverse of yearly mean flow of the Susquehanna River were
333 conducted, in which the flow (smoothed or unsmoothed) was shifted by different
334 numbers of days. A moving average of 360 days was applied to the flow in order to
335 remove the seasonal frequency. The result showed that the best relation was found when
336 the flow was smoothed and shifted by 83 days, with an R^2 value of 0.92 (Fig. 8). Without
337 smoothing, the largest R^2 value was 0.84 when the flow was shifted by 108 days (Fig. 8).
338 It should be noted that a shift of 83 days meant that the RT of a given time was
339 determined by the flow condition after that given time, instead of prior. For instance, the
340 yearly mean RT for 1980 ($t=0-365$ days) is determined by the yearly mean river
341 discharge of 83-448 days.

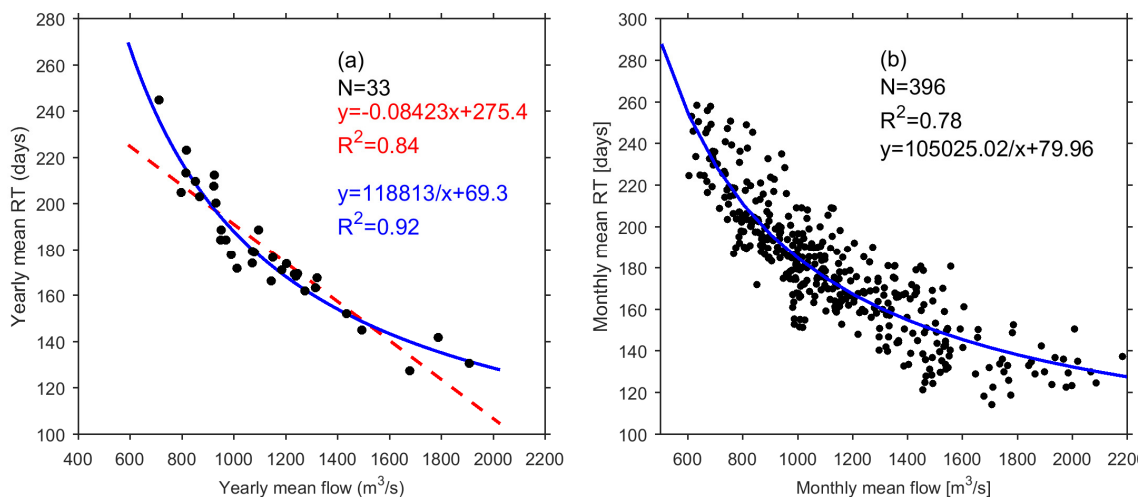
342 The best relation between yearly mean RT (days) averaged over the entire Bay and the
343 inverse of yearly mean flow (m^3/s) was shown in Eq. 4, where the flow was moving
344 averaged by 360 days and shifted by 83 days (Fig. 9a).

$$345 \quad RT = 118,813 / flow + 69.3, R^2 = 0.92, N = 33 \quad (4)$$

346 This significant relationship suggests that, when it was averaged yearly, the RT is
347 mainly controlled by river discharge and other factors (e.g. wind, tide) have little impact.
348 However, for a shorter period, the river discharge accounts for a much less percentage of
349 the variation of the RT. Even by shifting the flow by 83 days and applying a moving
350 average of 360 days, the river discharge accounts for 78% of the monthly mean RT
351 variation (Fig. 9b). Without smoothing of the river flow, there is no significant relation
352 between the monthly RT and the monthly flow, with the largest R^2 of only 0.22. This can

353 be understood as the variation of RT was between 110-264 days, and the RT depends on
 354 the accumulative effect of river flow and other factors (e.g., tide, wind, and the pre-
 355 existing condition)for a period of more than 110 days. A short-term pulse of river flow
 356 does not necessarily result in a significant change of RT, as the impact of the pulse can be
 357 confounded by varied flow conditions in the following days. Even though there were
 358 usually multiple pulses of high flow in each year, including short-term pulses (e.g.,
 359 during storm periods in the summer), there was usually only one peak and one trough of
 360 RT in each year (Fig. 6).

361



362

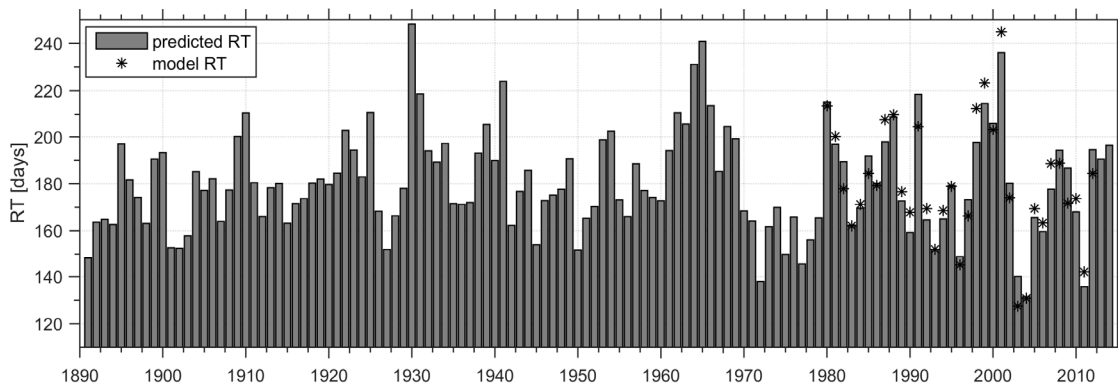
363 **Fig. 9.**(a) Regression between interannual variation of yearly mean residence time
 364 averaged over the entire Bay and interannual variation of yearly mean Susquehanna River
 365 flow shifted by 83 days and moving averaged by 360 days; two kinds of regression were
 366 applied and the correlation coefficient is shown in text, where the red dashed line denotes
 367 the linear regression between RT and flow, and the blue solid line denotes the linear
 368 regression between RT and 1/flow; (b) regression between monthly mean residence time

369 averaged over the entire Bay and monthly mean flow shifted by 83 days and moving
370 averaged by 360 days.

371

372 Based on the significant flow-RT relationship (Eq. 4), a long-term estimation of yearly
373 mean RT back to 1891 was conducted and shown in Fig. 10. The 360-day moving average
374 and the 83-day shifting of the flow were applied. Susquehanna River flow
375 data were those observations collected at USGS Station 01578310, which had daily
376 discharge data since 1967. The missing discharge data of 1891-1967 were estimated with
377 the data from another nearby Station USGS 01570500, located upstream of Station USGS
378 01578310. Daily discharge values measured at these two stations were highly linearly
379 correlated ($R^2=0.997$, from a 10-year linear regression). The estimation showed that RT
380 of the past century had a high variability. It seems the interannual variability became
381 larger after the 1970s. The maximum RT occurred in 1930 (RT=248 days) and the
382 minimum RT occurred in 2004 (RT=132 days). No significant trend could be found for
383 the past century.

384



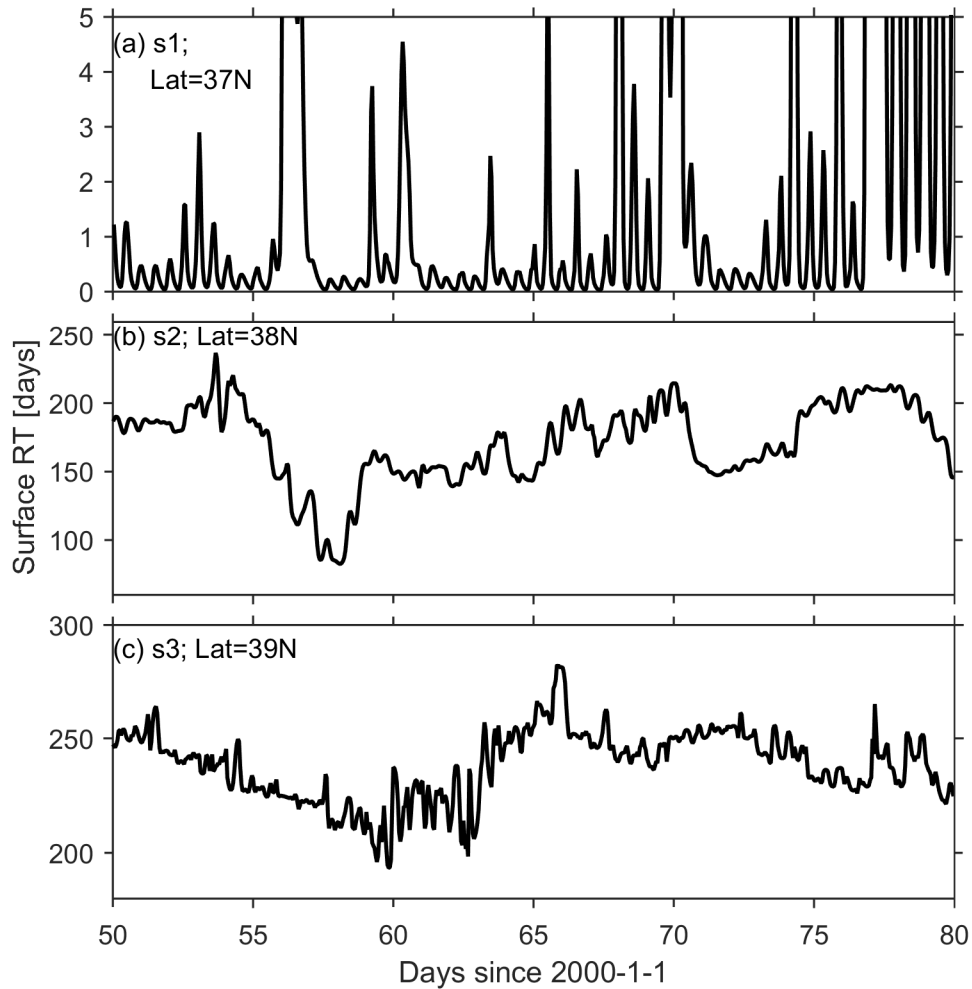
385

386 **Fig. 10.** Estimated mean residence time of the entire Bay since 1891; annual mean
387 residence time from model simulation is shown as a black asterisk.

388

389 **4.2 Impact of estuarine circulation on RT**

390 Despite the high correlation between the yearly mean RT and yearly mean flow, a
391 large part of the monthly RT variation remained to be explained. Besides the river
392 discharge, tidal exchange and estuarine circulation are two main processes that contribute
393 to the water exchange between an estuary and coastal waters. The relative importance of
394 tidal exchange and estuarine circulation differs in different systems (Hansen and Rattray,
395 1965; Officer and Kester, 1991). Tide has proven to be important to affect water transport
396 through tidal pumping (Chen et al., 2012) and thus change the pattern of the RT,
397 especially for a small estuary where RT is relatively small (Brye et al., 2012; Andutta et
398 al., 2016). In the Chesapeake Bay, tide contributes to the vertical mixing and the
399 formation of asymmetry of west-east RT distribution and to the gravitational circulation
400 that leads to the huge difference between surface and bottom RT. Consistent with the
401 findings of Brye et al. (2012), RT varied more significantly over a tidal cycle than over a
402 spring-neap cycle, especially in the area near the mouth boundary (Fig. 11). The semi-
403 diurnal tidal component of the RT weakens toward the upstream. No significant signal of
404 the spring-neap cycle in the RT time-series at selected stations was found. As the
405 residence time of the Bay is on the order of 100 days, the semi-diurnal tidal signal
406 becomes insignificant towards the upstream.



407

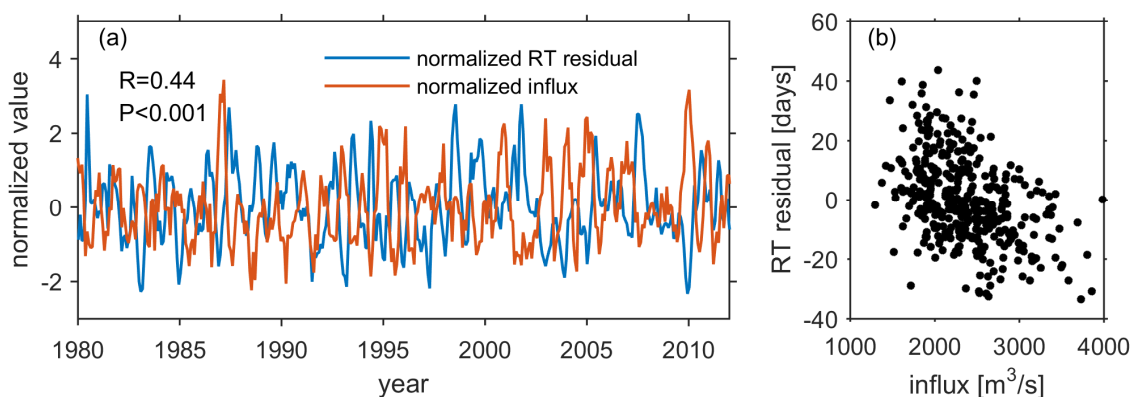
408 **Fig. 11.** Time-series of hourly mean surface residence time at 3 selected stations (i.e.
 409 s1, s2, s3), whose locations are shown in Fig. 1b.

410

411 The other important process that may have a significant impact on the RT is the
 412 estuarine circulation. Hagy et al. (2000) demonstrated the saline influx at the mouth of a
 413 partially mixed estuary is important to the water renewal, especially in the area near the
 414 mouth. To quantify the variability of estuarine circulation, we calculated the influx for
 415 each month at a mid-Bay cross-section (location shown in Fig. 1b with red line) to

416 indicate the strength of the circulation. In order to remove the impact of river discharge
417 on monthly mean RT, the residual value from the monthly RT-flow regression (Fig. 9b)
418 was used to compare with the monthly influx at the mid-Bay cross-section. Similar to the
419 regression between river flow and RT, a delay of 83 days was also considered when
420 conducting the regression between the residual and influx.

421



422

423 **Fig. 12.**(a) Time-series of normalized influx at the middle Bay cross section (red line)
424 and normalized residual value from the monthly RT-Flow regression (blue line). Both
425 time series were normalized by removing the mean and dividing by the standard deviation.
426 A positive value 1.0 of normalized influx denotes the influx is larger than the mean influx
427 by 1.0 standard deviation. (b) Scatter plot of the influx and residual value from the
428 monthly RT-Flow regression.

429

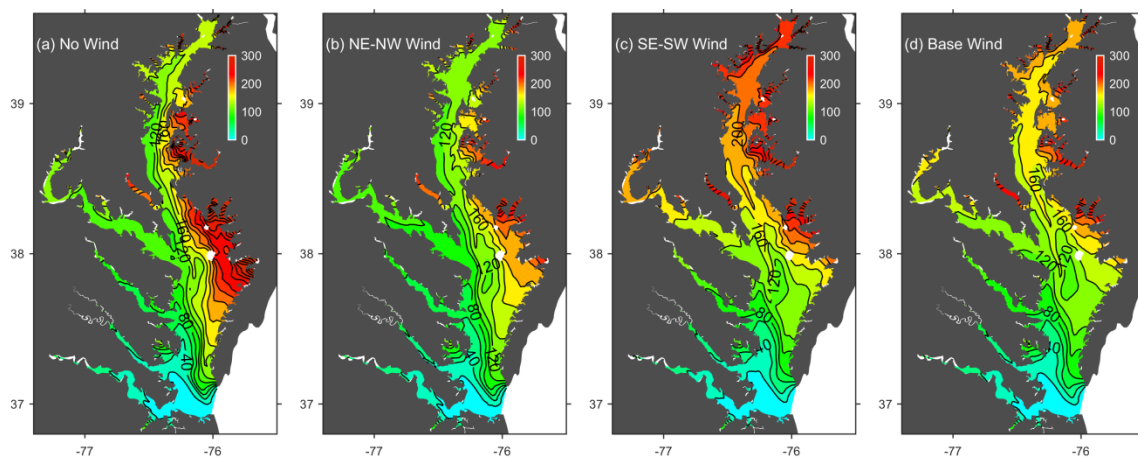
430 The regression between the residual and influx showed that the residual was highly
431 negatively correlated with the influx, with $p < 0.001$ (Fig. 12). Even though the R^2 is not
432 high, troughs of the residual RT often coincide with peaks of influx. A larger influx will

433 enhance the outflow and lead to a faster water exchange near the mouth and thus smaller
434 RT. This significant relation also suggests that those factors (e.g., wind, tide, river
435 discharge) affecting the estuarine circulation could also have potential impact on the RT,
436 especially on the short-term averaged RT.

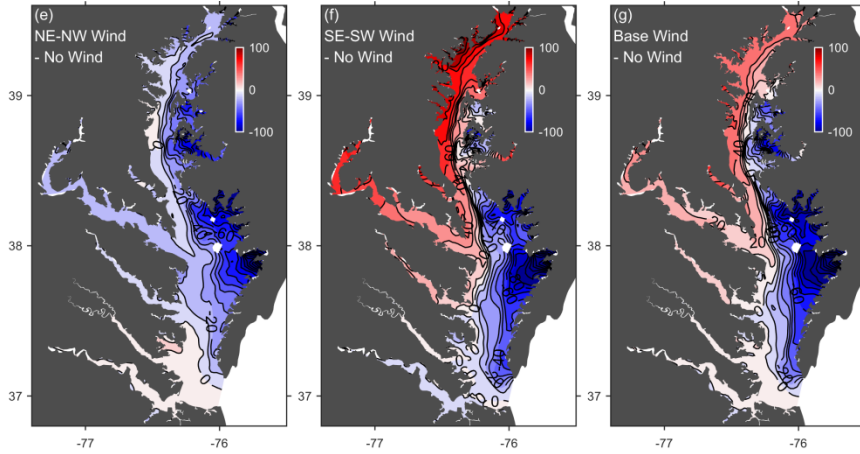
437 4.3 Impact of wind

438 The influence of wind on estuarine circulation has been recognized for many years
439 (Geyer, 1997; Guo and Valle-Levinson, 2008; Scully, 2010; Li and Li, 2011, 2012;
440 Officer, 1976; Scully, 2010; Wang, 1979). To examine the influence of wind on RT,
441 several numerical experiments were conducted (i.e., without wind, with NE-NW wind,
442 with SE-SW wind, base case with all directions of wind). For these simulations, model
443 runs were from 2002 to 2005 and the model configuration was unchanged except the
444 wind forcing. For example, in the NE-NW wind case, wind was set to be zero when there
445 is the SE or SW wind. The RT value of year 2003 was analyzed and compared.

446



447



448

449 **Fig. 13.** (a-d) Yearly and vertically averaged RT of 2003 under different wind forcing
 450 conditions. (e-f) The impact of wind forcing on the RT, indicated by the differences
 451 between model simulations with and without wind forcings.

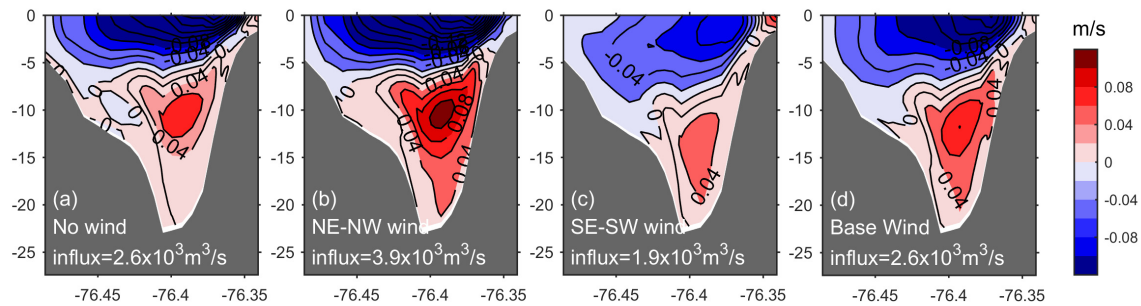
452

453 The comparison between different cases suggests that wind can have a significant
 454 impact on the lateral pattern of RT. With the NE-NW wind forcing, the RT distribution is
 455 very similar to the RT distribution without wind forcing, both with large lateral
 456 asymmetry between the eastern and western region in the mainstem (Fig.13a-b). The
 457 lateral asymmetry is most significant near the mouth of Potomac River (~38N). Southerly
 458 wind, however, generates a similar lateral pattern as under base wind condition, in which
 459 the asymmetry is highly weakened (Fig.13c-d).

460 The difference between the no-wind case and the other cases reveals that northerly
 461 wind and southerly wind have different impacts in different regions and their impacts are
 462 not simply opposite to each other. Both southerly and northerly winds are likely to reduce
 463 the RT in the eastern region of the lower-middle Bay (Fig. 13e-f). Southerly wind
 464 increase the RT in the middle-upper Bay significantly by up to 100 days (Fig. 13f), while

465 the northerly wind has little impact (<20 days) in the western region of the middle-upper
 466 Bay (Fig.13e). It appears that the southerly wind plays a more dominant role in
 467 controlling the long-term transport, which is consistent with findings for the impact of
 468 wind on freshwater age (Shen and Wang, 2007). The southerly wind causes strong lateral
 469 and vertical mixing, reduces the gravitational circulation, and thereby increases the
 470 transport time. The influx at the mid-Bay cross-section, indicating the strength of
 471 gravitational circulation, was strongly reduced by the SE-SW wind and enhanced by the
 472 NE-NW wind (Fig. 14). Compared to NE-NW wind, the influx was reduced by half with
 473 SE-SW wind.

474



475

476 **Fig. 14.** Along channel residual current at the middle Bay cross section under different
 477 wind forcing conditions, with contour level of 0.02 m/s (black lines). Positive value
 478 denotes an influx to the upstream. Values of laterally and vertically integrated influx are
 479 shown in the text at the bottom.

480

481 **5. Conclusion**

482 In this study we investigate the water exchange between the Chesapeake Bay and its
483 adjacent coastal sea, using the timescale residence time (RT) that can often be used to
484 evaluate the impacts of hydrodynamic conditions on biological and geochemical
485 processes. The long-term simulation of water RT of the Chesapeake Bay was conducted
486 over the period from 1980 to 2012, using an adjoint method, which enables us to compute
487 the time-varying RT in a single model run. The impacts of river discharge, intensity of
488 estuarine circulation, and wind on the RT were discussed. The main conclusions are
489 summarized as follows. (1) The vertically mean RT averaged over the entire Chesapeake
490 Bay system ranges from 110 to 264 days, with a mean of 180 days and a standard
491 deviation of 30 days over the past 3 decades. No clear trend was detected during the past
492 three decades. The bottom RT was larger than that of the surface due to the gravitational
493 circulation, and the vertical differences could be as large as 100 days. (2) There was a clear
494 seasonal cycle of RT, with high RT occurring in the summer and low RT occurring in the
495 winter, suggesting materials released in winter would be flushed out most quickly. (3)
496 Interannual variability of the RT was significant and was highly correlated with the
497 variability of river discharge. The correlation coefficient between yearly mean RT and
498 yearly mean river discharge can be as high as 0.92, if the river discharge was shifted by 83
499 days and a moving average of 360 days was applied. (4) The monthly variability of RT
500 can be partially attributed to the variability of estuarine circulation. A strengthened
501 estuarine circulation results in a larger bottom influx and thus reduces the RT. (5) Wind
502 exerts a significant impact on the lateral pattern of RT. The upstream wind is more
503 important in controlling the lateral pattern of RT in the mainstem than the downstream
504 wind.

505 **Acknowledgements**

506 We thank Mac Sisson for his assistance in editing the manuscript. We thank Mark Brush,
507 Carl Hershner, Kyeong Park, and Harry Wang for their suggestions. We are grateful to
508 Ya Wang, Qubin Qin and Xin Yu for their assistance in coding of the model and helpful
509 comments. This work is supported by the National Science Foundation (Award
510 #1325518). Additional support is provided by Virginia Institute of Marine Science. This
511 is contribution No. xxxxx of the Virginia Institute of Marine Science, School of Marine
512 Science, College of William and Mary, Virginia.

513

514 **References**

- 515 Alber, M., and J. E. Sheldon (1999), Use of a date-specific method to examine variability
516 in the flushing times of Georgia estuaries, *Estuarine, Coastal Shelf Sci.*, 49(4), 469–
517 482, doi:10.1006/ecss.1999.0515.
- 518 Andutta, F. P., F. Helfer, L. B. de Miranda, E. Deleersnijder, C. Thomas, and C.
519 Lemckert (2016), An assessment of transport timescales and return coefficient in
520 adjacent tropical estuaries, *Cont. Shelf Res.*, 124, 49–62,
521 doi:10.1016/j.csr.2016.05.006
- 522 Blaise S., B. de Brye, A. de Brauwere, E. Deleersnijder, E.J.M. Delhez, and R. Comblen,
523 (2010), Capturing the residence time boundary layer - Application to the Scheldt
524 Estuary, *Ocean Dynamics*, 60, 535-554
- 525 Bolin, B., and H. Rodhe (1973), A note on the concepts of age distribution and transit
526 time in natural reservoirs, *Tellus*, 25, 58–63, doi:10.1111/j.2153-
527 3490.1973.tb01594.x.
- 528 Boynton, W. R., J. H. Garber, R. Summers, and W. M. Kemp (1995), Inputs,
529 transformations, and transport of nitrogen and phosphorus in Chesapeake Bay and
530 selected tributaries, *Estuaries*, 18, 285–314, doi: 10.2307/1352640.
- 531 Brye, B. D., A. D. Brauwere, O. Gourgue, E. J. M. Delhez, and E. Deleersnijder (2012),
532 Water renewal timescales in the Scheldt Estuary, *J. Mar. Syst.*, 94, 74-86.
- 533 Carpenter, S. R., N. F. Caraco, D. L. Correll, R. W. Howarth, A. N. Sharpley, and V. H.
534 Smith (1998), Nonpoint pollution of surface waters with phosphorus and nitrogen,
535 *Ecol. Appl.*, 8(3), 559–568, doi: 10.1890/1051-
536 0761(1998)008[0559:NPOSWW]2.0.CO;2
- 537 Cerco, C., and T. Cole (1992), Application of the three-dimensional eutrophication
538 model.CE- QUAL-ICM to Chesapeake Bay. Draft Technical Report. U.S. Army
539 Engineer Waterways.
- 540 Chen, S, W. R. Geyer, D. K. Ralston, and J. A. Lerczak (2012), Estuarine exchange flow
541 quantified with isohaline coordinates: contrasting long and short estuaries, *J. Phys.*
542 *Oceano.*, 42, 748-763.
- 543 Deleersnijder, E., J. M. Campin, and E. J. M. Delhez (2001), The concept of age in
544 marine modeling, I. Theory and preliminary model results, *J. Mar. Syst.*, 28, 229–267,
545 doi:10.1016/S0924-7963(01)00026-4.
- 546 Delhez, E. J. M., A. W. Heemink, and E. Deleersnijder (2004), Residence time in a semi-
547 enclosed domain from the solution of an adjoint problem, *Estuarine, Coastal Shelf*
548 *Sci.*, 61, 691–702, doi:10.1016/j.ecss.2004.07.013.

- 549 Delhez, E. J. M. (2005), Transient residence and exposure times, *Ocean Sci.*, 2(3), 1–9,
550 doi:10.5194/os-2-1-2006.
- 551 Delhez E.J.M. and E. Deleersnijder, (2006), The boundary layer of the residence time
552 field, *Ocean Dynamics*, 56, 139-150.
- 553 Dettmann, E. H. (2001), Effect of water residence time on annual export and
554 denitrification of nitrogen in Estuaries: a model analysis, *Estuaries*, 24(4), 481-490,
555 doi:10.2307/1353250.
- 556 Du, J., and J. Shen (2015), Decoupling the influence of biological and physical processes
557 on the dissolved oxygen in the Chesapeake Bay, *J. Geophys. Res.*, 120, 78–93,
558 doi:10.1002/jgrc.20224.
- 559 Dyer, K. R. (1973), *Estuaries: a Physical Introduction*, John Wiley & Sons, New York.
- 560 Geyer, W. R. (1997), Influence of wind on dynamics and flushing of shallow estuaries,
561 *Estuarine, Coastal Shelf Sci.*, 44, 713-722.
- 562 Geyer, W. R., J. T. Morris, F. G. Pahl, and D. A. Jay (2000), Interaction between physical
563 processes and ecosystem structure: a comparative approach, in *Estuarine Science: a*
564 *Synthetic Approach to Research and Practice*, edited by J. E. Hobbie, pp177-210,
565 Island Press, Washington, DC.
- 566 Gong, W., J. Shen, and J. Jia (2008), The impact of human activities on the flushing
567 properties of a semi-closed lagoon, Xiaohai, Hainan, China, *Mar. Environ. Res.*, 65,
568 62-76, doi: 10.1016/j.marenvres.2007.08.001.
- 569 Goodrich, D. M. (1988), On meteorologically induced flushing in three U.S. east coast
570 estuaries, *Estuarine, Coastal Shelf Sci.*, 26, 111–121, doi:10.1016/0272-
571 7714(88)90045-5.
- 572 Guo, X., and A. Valle-Levinson (2007), Tidal effects on estuarine circulation and outflow
573 plume in the Chesapeake Bay, *Cont. Shelf Res.*, 27(1), 20–42,
574 doi:10.1016/j.csr.2006.08.009.
- 575 Guo, X., and A. Valle-Levinson (2008), Wind effects on the lateral structure of density-
576 driven circulation in Chesapeake Bay, *Cont. Shelf Res.*, 28, 2450-2471
- 577 Hagy, J. D., L. P. Sanford, and W. R. Boynton (2000), Estimation of net physical
578 transport and hydraulic residence times for a coastal plain estuary using box models,
579 *Estuaries*, 23, 328-340, doi: 10.2307/1353325.
- 580 Hamrick, J. M. (1992), A three-dimensional environmental fluid dynamics computer
581 code: theoretical and computational aspects (Special Report in Applied Marine

- 582 Science and Ocean Engineering. No. 317), Virginia Institute of Marine Science, The
583 College of William and Mary, Gloucester Point.
- 584 Hansen, D. V., and M. Rattray (1965), Gravitational circulation in straits and estuaries, *J.*
585 *Mar. Res.*, 23, 104-122.
- 586 Hong, B., and J. Shen (2012), Responses of estuarine salinity and transport processes to
587 potential future sea-level rise in the Chesapeake Bay, *Estuarine, Coastal Shelf Sci.*,
588 104-105, 33–45, doi:10.1016/j.ecss.2012.03.014.
- 589 Hong, B., and J. Shen (2013), Linking dynamics of transport timescale and variations of
590 hypoxia in the Chesapeake Bay, *J. Geophys. Res.: Oceans*, 118(February), 6017–
591 6029, doi:10.1002/2013JC008859.
- 592 Huang, W., X. Liu, X. Chen, and M. S. Flannery (2010), Estimating river flow effects on
593 water ages by hydrodynamic modeling in Little Manatee River estuary Florida, USA,
594 *Environ. Fluid Mech.*, 10, 297-211, doi:10.1007/s10652-009-9143-6.
- 595 Josefson, A. B., and B. Rasmussen (2000), Nutrient retention by benthic macrofaunal
596 biomass of Danish Estuaries: importance of nutrient load and residence time,
597 *Estuarine Coastal Shelf Sci.*, 50, 205–216, doi:10.1006/ecss.1999.0562.
- 598 Kemp, W. M., W. R. Boynton, J. E. Adolf, D. F. Boesch, W. C. Boicourt, and G. Brush
599 (2005), Eutrophication of Chesapeake Bay : historical trends and ecological
600 interactions, *Mar. Ecol. Prog. Ser.*, 303, 1–29, doi: 10.3354/meps303001.
- 601 Kennish, M. J. (1997), Practical Handbook of Estuarine and Marine Pollution, pp. 524,
602 CRC Press, Boca Raton.
- 603 Li, Y., and M. Li(2011), Effects of winds on stratification and circulation in a partially
604 mixed estuary, *Journal of Geophysical Research: Oceans*, 116(12).
605 doi:10.1029/2010JC006893
- 606 Li, Y., and M. Li(2012), Wind-driven lateral circulation in a stratified estuary and its
607 effects on the along-channel flow, *J. Geophys. Res.: Oceans*, 117(C9).
608 doi:10.1029/2011JC007829
- 609 Lindahl, O., A. Belgrano, L. Davidsson, and B. Hernroth (1998), Primary production,
610 climatic oscillations, and physico-chemical processes: the Gullmar Fjord time-series
611 data set (1985-1996), *ICES J. Mar. Sci.*, 55(4), 723–729,
612 doi:10.1006/jmsc.1998.0379.
- 613 Liu, W., W. Chen, and J. Kuo (2008), Modeling residence time response to freshwater
614 discharge in a mesotidal estuary, Taiwan, *J. Mar. Sys.*, 74, 295-314, doi:
615 10.1016/j.jmarsys.2008.01.001.

- 616 Liu, Z., H. Wei, G. Liu, and J. Zhang (2004), Simulation of water exchange in Jiaozhou
617 Bay by average residence time approach, *Estuarine, Coastal Shelf Sci.*, 61, 25–35,
618 doi:10.1016/j.ecss.2004.04.009.
- 619 Monbet, Y. (1992), Control of phytoplankton biomass in estuaries: a comparative
620 analysis of microtidal and macrotidal estuaries, *Estuaries*, 15, 563–571,
621 doi:10.2307/1352398.
- 622 Mosen, N. E., J. E. Cloern, L. V. Lucas, and S. G. Monismith (2002), The use of
623 flushing time, residence time, and age as transport time scales, *Limnol.*
624 *Oceanogr.*, 47(5), 1545–1553, doi:10.4319/lo.2002.47.5.1545.
- 625 Murphy, R. R., W. M. Kemp, and W. P. Ball (2011), Long-term trends in Chesapeake
626 Bay seasonal hypoxia, stratification, and nutrient loading, *Estuaries and Coasts*,
627 34(6), 1293-1309, doi:10.1007/s12237-011-9413-7.
- 628 Nixon, S. W. (1995), Coastal marine eutrophication: A definition, social causes, and
629 future concerns, *Ophelia*, 41(1), 199-219, doi: 10.1080/00785236.1995.10422044.
- 630 Nixon, S. W., J. W. Ammerman, L. P. Atkinson, V. M. Berounsky, G. Billen, W. C.
631 Boicourt, W. R. Boynton, T.M. Church, D. M. Ditoro, R. Elmgren, J. H. Garber, A.
632 E. Giblin, R. A. Jahnke, N. J. P. Owens, M. E. Q. Pilson, and S. P. Seitzinger (1996),
633 The fate of nitrogen and phosphorus at the land-sea margin of the North Atlantic
634 Ocean, *Biogeochemistry*, 35(1), 141–180, doi:10.1007/BF02179826.
- 635 Nordberg, K., H. L. Filipsson, M. Gustafsson, R. Harland, and P. Roos (2001), Climate,
636 hydrographic variations and marine benthic hypoxia in Koljo Fjord, Sweden, *J. Sea*
637 *Res.*, 46(3-4), 187-200, doi: 10.1016/S1385-1101(01)00084-3.
- 638 Officer, C.B. (1976), *Physical Oceanography of Estuaries (and Associated Coastal*
639 *Waters)*, pp. 465, Wiley, New York
- 640 Officer, C. B., and D. R. Kester (1991), On estimating the non-advective tidal exchanges
641 and advective gravitational circulation exchanges in an estuary, *Estuarine, Coastal*
642 *Shelf Sci.*, 32(1), 99–103. doi:10.1016/0272-7714(91)90031-6.
- 643 Oliveira, A., and A. M. Baptista (1997), Diagnostic modeling of residence times in
644 estuaries, *Water Resour. Res.*, 33(8), 1935–1946, doi:10.1029/97WR00653.
- 645 Paerl, H. W., L. M. Valdes, B. L. Peierls, J. E. Adolf, and L. W. Harding (2006),
646 Anthropogenic and climatic influences on the eutrophication of large estuarine
647 ecosystems, *Limnol. Oceanogr.*, 51(1_part_2), 448–462,
648 doi:10.4319/lo.2006.51.1_part_2.0448.
- 649 Rosenberg, R. (1990), Negative oxygen trends in Swedish coastal bottom waters, *Mar.*
650 *Pollut. Bull.*, 21(7), 335–339, doi:10.1016/0025-326X(90)90794-9.

- 651 Scully, M. E. (2010), Wind Modulation of Dissolved Oxygen in Chesapeake Bay,
652 *Estuaries and Coasts*, 33(5), 1164–1175. doi:10.1007/s12237-010-9319-9.
- 653 Shen, J., and L. Haas (2004), Calculating age and residence time in the tidal York River
654 using three-dimensional model experiments, *Estuarine, Coastal Shelf Sci.*, 61(3),
655 449–461, doi: 10.1016/j.ecss.2004.06.010.
- 656 Shen, J., and H. V. Wang (2007), Determining the age of water and long-term transport
657 timescale of the Chesapeake Bay, *Estuarine, Coastal Shelf Sci.*, 74(4), 750–763,
658 doi:10.1016/j.ecss.2007.05.017.
- 659 Smith, V. H., G. D. Tilman, and J. C. Nekola (1999), Eutrophication: Impacts of excess
660 nutrient inputs on freshwater, marine, and terrestrial ecosystems, *Environ.*
661 *Pollut.*, 100(1-3), 179–196, doi:10.1016/S0269-7491(99)00091-3.
- 662 Takeoka, H. (1984), Fundamental concepts of exchange and transport time scales in a
663 coastal sea, *Cont. Shelf Res.*, 3(3), 311–326, doi:10.1016/0278-4343(84)90014-1.
- 664 Valle-Levinson, A., C. Reyes, and R. Sanay (2003), Effects of bathymetry, friction, and
665 rotation on estuary–ocean exchange, *J. Phys. Oceanogr.*, 33(i), 2375–2393,
666 doi:10.1175/1520-0485(2003)033<2375:EOBFAR>2.0.CO;2.
- 667 Wang, D. P. (1979), Wind-driven circulation in the Chesapeake Bay, winter 1975, *J.*
668 *Phys. Oceanogr.*, 9, 564–572.
- 669 Wang, C. F., M. H. Hsu, and A. Y. Kuo (2004), Residence time of the Danshuei River
670 estuary, Taiwan, *Estuarine, Coastal Shelf Sci.*, 60, 381–393,
671 doi:10.1016/j.ecss.2004.01.013.
- 672 Wang, T., and Z. Yang (2015), Understanding the flushing capability of Bellingham Bay
673 and its implication on bottom water hypoxia, *Estuarine, Coastal Shelf Sci.*, (May),
674 1–12, doi:10.1016/j.ecss.2015.04.010.
- 675 Wong, K.C., and A. Valle-Levinson (2002), On the relative importance of the remote and
676 local wind effects on the subtidal exchange at the entrance to the Chesapeake Bay, *J.*
677 *Mar. Res.*, 60, 477–498. doi:10.1357/002224002762231188.
- 678 Zimmerman, J. T. F. (1976), Mixing and flushing of tidal embayments in the western
679 Dutch Wadden Sea Part I: Distribution of salinity and calculation of mixing time
680 scales, *Neth. J. Sea Res.*, 10(2), 149–191, doi:10.1016/0077-7579(76)90013-2.
- 681